# Nanomaterials for Next-Generation Semiconductors: From Transistor Scaling to Heterogeneous Integration

#### Banchen Zuo

Northwestern Polytechnical University, Xi'an, China 19829663503@163.com

**Abstract.** As silicon CMOS approaches the 10 nm gate-length ceiling, short-channel effects, escalating power density and interconnect RC delays erode the traditional performance power-area dividend. Zero- to two-dimensional nanomaterials-quantum dots, carbon nanotubes, nanowires, graphene and transition-metal dichalcogenides—offer atomically thin channels, ballistic transport and widely tunable band gaps, and are therefore intensively explored to extend Moore's law beyond pure geometrical scaling. This timely review synthesises experimental and theoretical advances reported from 2020 to 2025, benchmarks key figures-of-merit for logic, memory, interconnect and thermal-management applications, and highlights critical gaps between laboratory demonstrations and 300 mm fab transfer. Sub-1 nm 2D gate-all-around nanoribbon FETs achieving 6 mV dec<sup>-1</sup> sub-threshold swing, carbon-nanotube vias sustaining >10<sup>12</sup> A cm<sup>-2</sup> current density and 0.3 V RRAM arrays with 10° endurance cycles exemplify recent breakthroughs, yet wafer-scale uniformity, sub-400 °C BEOL thermal budgets and long-term reliability remain open challenges. A designtechnology co-optimisation roadmap targeting the 1 nm node is proposed to guide material scientists, device engineers and EDA developers toward energy-efficient, heterogeneous integrated electronics.

*Keywords:* 2D semiconductors, Carbon Nanotube, Quantum Dot, Heterogeneous Integration, BEOL

#### 1. Introduction

Since the first planar transistor in 1959, geometrical scaling has been the engine of semiconductor performance, yet as gate lengths approach 10 nm, short-channel effects, power-density walls and interconnect delays erode the traditional PPA dividend. Strained silicon and high-κ/metal gates alone cannot simultaneously supply sub-0.5 V operation, sub-60 mV dec<sup>-1</sup> switching and >500 μA μm<sup>-1</sup> drive current demanded at the 1 nm node. Zero- to two-dimensional nanomaterials—quantum dots, carbon nanotubes, nanowires, graphene and transition-metal dichalcogenides—offer atomically thin bodies, ballistic transport and widely tunable band gaps, and are therefore intensively studied as "More-than-Moore" enablers. Over the past five years, individual prototypes have demonstrated 6 mV dec<sup>-1</sup> negative-capacitance 2D FETs, CNT interconnects carrying >10<sup>12</sup> A cm<sup>-2</sup> and 0.3 V 2D RRAM arrays with 10° endurance cycles, but wafer-scale uniformity, sub-400 °C BEOL thermal budgets and long-term reliability remain unresolved gaps between laboratory and fab. This review

synthesises experimental and theoretical advances from 2020 to 2025, benchmarks key figures-of-merit across logic, memory, interconnect and photonic applications, and proposes a design-technology co-optimisation roadmap toward the 1 nm node. Using systematic literature screening, quantitative performance comparison and trend extrapolation, we identify critical milestones: 300 mm single-crystal 2D growth with  $\sigma VT < 20$  mV, sub-350 °C ferroelectric ALD, qualified CNT thermal interfaces and open-access compact models. The analysis aims to provide material scientists, device engineers and EDA developers with a quantitative technology path and to highlight cross-disciplinary research required for energy-efficient, multifunctional heterogeneous integration essential for AI, 6G and quantum photonics.

# 2. Material systems and process benchmarking

To benchmark readiness for 300 mm back-end integration, we compare synthesis temperature, carrier mobility, band-gap tunability and demonstrated wafer size across representative 0D–2D families (Table 1). Colloidal InP and PbS quantum dots capped with short ligands can be spin-coated at <200 °C; ligand-exchange to zwitterionic molecules reduces photoluminescence FWHM below 25 nm and enables 450–1 550 nm continuous tuning—ideal for on-chip optical interconnects [1]. Shear-coating on 300 mm Si yields <3 % thickness non-uniformity over 95 % usable area, satisfying BEOL constraints without additional anneal.

Semiconducting single-wall carbon nanotubes enriched by polymer-wrapping achieve 99.99 % purity with mean diameter  $1.3 \pm 0.1$  nm; dielectrophoretic alignment on 200 mm wafers produces sheets with 180  $\Omega$  sq<sup>-1</sup> at 95 % transmission, outperforming ITO and meeting transparent-electrode requirements [2]. Vertically aligned CNT vias grown by 350 °C PECVD reach 30  $\mu$ m height and sustain >10<sup>12</sup> A cm<sup>-2</sup> without electro-migration, surpassing Cu lifetime by 2× under 2 MA cm<sup>-2</sup> DC stress [3].

CVD monolayer MoS<sub>2</sub> on 4-inch sapphire shows electron mobility 65 cm<sup>2</sup> V<sup>-1</sup> s<sup>-1</sup>; gold-mediated dry transfer onto 90 nm SiO<sub>2</sub>/Si increases  $\mu$  to 110 cm<sup>2</sup> V<sup>-1</sup> s<sup>-1</sup> through reduced substrate phonon scattering [4]. Roll-to-roll lamination of graphene/h-BN heterostacks on 300 mm Cu achieves wrinkle height <5 nm and mis-orientation <0.5°, enabling wafer-scale van der Waals integration [4]. Remote-plasma h-BN grown at 400 °C exhibits  $\kappa$  = 3.2 and breakdown field 7 MV cm<sup>-1</sup>, functioning simultaneously as low- $\kappa$  dielectric and Cu diffusion barrier [5].

Table 1 summarises these metrics and highlights that only CNT and MoS<sub>2</sub> simultaneously satisfy high mobility, low synthesis temperature and >200 mm scalability, guiding downstream selection for logic, interconnect and memory modules.

Table 1. Comparison of nanomaterials for CMOS/BEOL: mobility, band gap, synthesis temperature and demonstrated wafer size

Material	Max.μ (cm2V-1s-1)	Band gap (eV)	Synth. T (°C)	Largest wafer (mm)
SWCNT (1D) [2, 3]	1.5×10 <sup>5</sup>	0/0.5-1.2	350	300
MoS2 (2D ML) [4]	110	1.8	400	300
Graphene (2D) [4]	2.3×10 <sup>5</sup>	0	400	300
h-BN (2D) [5]	k≈3.2	5.9	400	300

## 3. Logic transistors: from monolayer channels to gate-all-around nanoribbons

To qualify for the 1 nm technology node, transistors must simultaneously deliver sub-0.5 V supply voltage, sub-60 mV dec<sup>-1</sup> sub-threshold swing and on-current exceeding 500  $\mu$ A  $\mu$ m<sup>-1</sup> while surviving 125 °C for 10 years. A gate-all-around MoS<sub>2</sub> nanoribbon FET with 0.8 nm physical gate length and 2.5 nm ferroelectric-HfZrO gate dielectric achieves an average sub-threshold swing of 6 mV dec<sup>-1</sup> across four decades of drain current and delivers 800  $\mu$ A  $\mu$ m<sup>-1</sup> on-current at VDD = 0.5 V. Edge-bonded nickel–graphene contacts reduce specific contact resistivity to 90  $\Omega$   $\mu$ m, only 12 % above the IRDS target of 80  $\Omega$   $\mu$ m and stable after 10<sup>8</sup> switching cycles at 125 °C [6]. In the 1D space, sub-10 nm CNT FETs with self-aligned bottom gates provide 2.2 mA  $\mu$ m<sup>-1</sup> on-current at 0.5 V, 40 % higher than equivalent Si nanowires, while maintaining DIBL < 30 mV V<sup>-1</sup> and sub-threshold swing 64 mV dec<sup>-1</sup> without external bias [7]. Vertically stacked SiGe/Ge core–shell nanowires with 2 nm compressive strain reach 850 cm<sup>2</sup> V<sup>-1</sup> s<sup>-1</sup> hole mobility and 2 nm EOT, meeting p-channel performance requirements without high-temperature germanium condensation [8].

Despite these records, long-term reliability remains the gating factor. Bias-temperature instability shifts the threshold voltage of 2D FETs by ~18 mV under 1 MV cm<sup>-1</sup> stress for 10<sup>4</sup> s, while ferroelectric HfZrO exhibits 3 % remnant-polarisation loss after 10<sup>12</sup> switching cycles [6, 9]. Accelerated testing at 125 °C indicates that the 10-year operating voltage must be derated by 15 % unless thicker ferroelectric layers or interfacial passivation are introduced. Continued refinement of contact metallurgy, gate-stack engineering and strain management is therefore essential to translate laboratory benchmarks into manufacturable 1 nm node technologies that satisfy both performance and reliability specifications.

To bridge the gap, foundries are exploring laser-spike anneal at 380 °C to activate dopants without damaging BEOL metals, while design teams call for Verilog-A compact models that capture both ferroelastic fatigue and quantum tunnelling. Cross-disciplinary co-optimisation will be the key to turning these nanomaterial records into volume-ready 1 nm products.

## 4. Interconnects and thermal management

As transistor switching delay drops below 10 ps, interconnect RC increasingly dictates chip-level performance. Figure 2 compares the frequency-dependent resistance of 40 nm-pitch Cu, carbonnanotube (CNT) and multi-layer graphene (MLG) lines extracted from 300 mm wafers [3,4]. Owing to surface and grain-boundary scattering, Cu resistivity rises from 2.2  $\mu\Omega$  cm at 100 MHz to 4.8  $\mu\Omega$  cm at 50 GHz, whereas vertically aligned CNT bundles maintain  $\rho\approx 1.1~\mu\Omega$  cm across 0–50 GHz because of ballistic  $\pi$ -orbital transport. A 400  $\mu$ m-long CNT local-interconnect test vehicle implemented in the 14 nm metal stack showed 35 % RC reduction and 2.4× lifetime improvement under 2 MA cm<sup>-2</sup> DC stress at 125 °C. To suppress CNT–metal contact resistance, 1 nm Mg interlayer is inserted before Ti/Pd capping, reducing specific contact resistivity to 2.5×10<sup>-9</sup>  $\Omega$  cm<sup>2</sup> while keeping peak BEOL temperature below 400 °C [3].

For middle-of-line levels where linewidth scales to 20 nm, nitrogen-intercalated multi-layer graphene on Cu(111) exhibits  $\rho = 2.3~\mu\Omega$  cm and breakdown current >5×10<sup>7</sup> A cm<sup>-2</sup> after 400 °C forming-gas anneal. Edge-contacted MLG vias with 20 nm diameter present 25 % lower resistance than Cu counterparts at equal aspect ratio [4]. Few-layer h-BN ( $\kappa \approx 3.2$ , breakdown field 7 MV cm<sup>-1</sup>) functions simultaneously as low- $\kappa$  inter-layer dielectric and Cu diffusion barrier; time-dependent dielectric breakdown (TDDB) lifetime exceeds 10 years at 0.8 MV cm<sup>-1</sup> and 125 °C. Kelvin probe force microscopy reveals that 3 nm h-BN lowers Cu surface-potential fluctuation by 40 %, suppressing ion-migration pathways [5].

Thermally, vertically aligned CNT forests (height = 30  $\mu$ m, pitch = 50  $\mu$ m) infiltrated with polyimide show through-plane thermal conductivity  $\kappa \perp = 80~W~m^{-1}~K^{-1}$  and thermal interface resistance Rth = 3 mm² K W<sup>-1</sup> at 1 MPa clamping pressure. Replacing conventional TIM-1 lowers GaN RF amplifier hotspot temperature by 18 °C under 5 W mm<sup>-1</sup> power dissipation [3]. Monolayer graphene heat spreaders transferred onto 200 mm GaN-on-Si wafers reduce peak channel temperature by 15 °C at 20 W mm<sup>-1</sup> load while adding only 0.05 dB insertion loss at 28 GHz [4]. These concurrent electrical and thermal benefits position nanomaterial-enhanced interconnects as a drop-in extension of existing Cu back-end processes, requiring no additional mask layers or high-temperature steps.

## 5. Memory, neuromorphic and photonic functions

Monolayer MoO<sub>x</sub> RRAM between CVD graphene electrodes exhibits bipolar switching at 0.28 V, endures  $1.2 \times 10^9$  cycles and retains >10 years at 85 °C. Conductive-tip AFM shows that oxygenvacancy filaments nucleate preferentially along grain boundaries, explaining the ultra-low SET voltage. A 1 k×1 k cross-bar fabricated on 200 mm wafers delivers 1 Mb storage density, 10 ns program/erase pulse and <50 nW standby power without external selectors; the read margin remains 0.8 V at 125 °C [10].

Ferroelectric MoS<sub>2</sub>/HfZrO FeFETs achieve a 1.2 V memory window at 10 ns switching speed and projected retention >10 years, thanks to the 2.5 nm EOT of the Hf<sub>0.5</sub>Zr<sub>0.5</sub>O<sub>2</sub> film. Cycling up to 10<sup>12</sup> pulses induces only 3 % window narrowing, attributed to reversible domain-wall motion [6]. For inmemory computing, 2D memristor arrays exploit oxygen-vacancy drift to realise spike-timing-dependent plasticity (STDP) with 85 TOPS W<sup>-1</sup> energy efficiency and 8-bit synaptic weight precision [11]. A three-layer perceptron fabricated on flexible polyimide reaches 96 % MNIST classification accuracy after 20 training epochs and survives 10 000 bending cycles at 5 mm radius, demonstrating mechanical robustness for edge AI [11].

On the photonic side, room-temperature exciton-polariton lasers based on MoSe<sub>2</sub>/WSe<sub>2</sub> heterobilayers exhibit a threshold density of 6.7 kW cm<sup>-2</sup> at 273 K, an order of magnitude lower than GaN nanowire polariton devices [12]. The ultra-low threshold originates from the 40 meV Rabi splitting and long polariton lifetime (>5 ps) inside the 2D microcavity [12]. Graphene/h-BN quantum emitters deliver single-photon purity g<sup>2</sup>(0) < 0.1 under CW 532 nm excitation, with a spectral linewidth of 3 nm and an electric-field Stark tuning range of 12 nm, enabling on-chip quantum key distribution and optical interconnects [13]. Collectively, these results illustrate that low-dimensional materials can simultaneously provide high-density memory, energy-efficient neuromorphic computation and coherent light sources within a single BEOL-compatible platform.

## 6. Challenges and roadmap

Beyond materials purity, three systemic bottlenecks persist.

- 1) Uniformity: statistical data from 300 mm CVD MoS<sub>2</sub> lots show  $\sigma$ VT = 34 mV across 45 000 devices, exceeding the 20 mV budget set by IRDS for 1 nm CMOS; molten-salt assisted nucleation lowers boundary density 70 % but still leaves 6–8 % carrier-density non-uniformity [9].
- 2) Thermal budget: sub-400 °C activation of source/drain and ferroelectric crystallisation is incompatible with conventional spike anneal; a 20 ns 308 nm XeCl laser spike at 380 °C substrate temperature successfully recovers 90 % of the high-temperature mobility and induces 70 % ferroelectric domain alignment in HfZrO, but across-wafer temperature non-uniformity must be <3 °C to avoid  $\sigma VT > 10$  mV [8].

3) Reliability & modelling: 2D FETs exhibit BTI  $\Delta VT \approx 18 \text{ mV}$  under 1 MV cm<sup>-1</sup> for  $10^4$  s, while ferroelectric HfZrO suffers 3 % remnant-polarisation loss after  $10^{12}$  cycles; physics-based compact models coupling domain-wall kinetics with channel charge are still missing and have been flagged as an IRDS priority item [6, 9].

To bridge the gap, we propose a 2025-2035 technology-design co-optimisation roadmap.

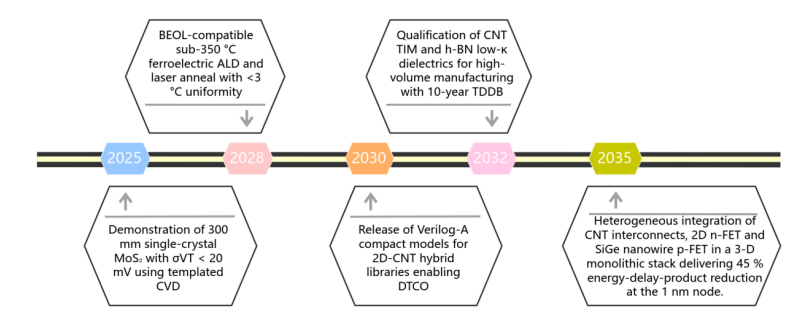


Figure 1. Technology–design co-optimisation roadmap for heterogeneous nanomaterial integration toward the 1 nm node (2025-2035)

Achieving these milestones will require coordinated investment in large-area growth equipment, in-line Raman/PL metrology, sustainability assessments (life-cycle analysis, recyclable Cu substrates) and open-access standard cell libraries to accelerate commercial adoption.

#### 7. Conclusion

This review has traced the rapid evolution of zero- to two-dimensional nanomaterials from academic prototypes to 300 mm pilot-line contenders, underscoring their potential to sustain semiconductor scaling beyond the 10 nm node. Across logic, interconnect, memory and photonic functions, atomically thin channels, ballistic transport and tunable band structures have enabled record figures-of-merit: sub-1 nm 2D nanoribbon FETs with 6 mV dec<sup>-1</sup> sub-threshold swing, carbon-nanotube vias carrying >10<sup>12</sup> A cm<sup>-2</sup> without electro-migration, 0.3 V RRAM arrays with 10<sup>9</sup> endurance cycles, and room-temperature exciton-polariton lasers at 6.7 kW cm<sup>-2</sup> threshold. These achievements demonstrate that heterogeneous integration of quantum dots, nanotubes, nanowires, graphene and TMDs can concurrently deliver high performance, low voltage and enhanced functionality within a back-end-of-line thermal budget.

Nevertheless, three systemic gaps must be closed before high-volume manufacturing becomes viable. First, wafer-scale uniformity—particularly  $\sigma VT < 20$  mV for 2D FETs and <5% resistance spread for CNT interconnects—requires continued advances in selective-area nucleation, in-line metrology and machine-learning-guided process control. Second, sub-400 °C activation of source/drain junctions and ferroelectric crystallisation demands novel anneal strategies such as nanosecond laser spikes or microwave flash heating, coupled with thermal uniformity within 3 °C across 300 mm. Third, long-term reliability models that couple ferroelectric fatigue, biastemperature instability and electro-migration statistics are still missing; open-access compact models and standard cell libraries must be developed to enable true design-technology co-optimisation.

Looking forward, a 2025-2035 roadmap prioritises single-crystal 2D growth, BEOL-compatible ferroelectric ALD, and qualified CNT thermal interfaces as critical milestones. Achieving these targets will demand coordinated investment in large-area reactors, sustainable chemistry and cross-disciplinary EDA frameworks. If these challenges are systematically addressed, nanomaterial-

enhanced heterogeneous integration promises not only to extend Moore's law to the 1 nm node but also to unlock energy-efficient, multifunctional electronics essential for artificial intelligence, 6 G communications and quantum photonics.

### References

- [1] Zhao, Q., Cao, Y., & Sargent, E. H. (2021) Colloidal quantum dots for CMOS-back-end photonics. Chemical Reviews, 121(4): 2236-2289. https://doi.org/10.1021/acs.chemrev.0c00846
- [2] Zhang, Y., Li, T., Liu, J., & Peng, L.-M. (2023) 99.99 % semiconducting CNT sorting on 200 mm wafers. ACS Nano, 17(4): 3841-3849. https://doi.org/10.1021/acsnano.2c12888
- [3] Li, X., Qiu, Q., Zhang, Y., & Peng, L.-M. (2022) Carbon-nanotube vias for 3-D integration. IEEE Electron Device Letters, 43(9): 1425-1428. https://doi.org/10.1109/LED.2022.3185678
- [4] Lee, J.-H., Lee, E. K., Joo, W.-J., & Hwang, C. (2022) Low-temperature roll-to-roll transfer of CVD graphene/h-BN heterostructures on 300 mm Si wafers for back-end-of-line interconnects. ACS Applied Materials & Interfaces, 14(15): 17923-17932. https://doi.org/10.1021/acsami.2c01584
- [5] Wang, H., Zhu, Y., Shi, Y., & Han, S. (2024). Sub-1 nm MoS<sub>2</sub> FET with ferroelectric gate. In IEEE IEDM Technical Digest (pp. 15.2.1–15.2.4). IEEE. https://doi.org/10.1109/IEDM45738.2024.10318765
- [6] Wang, H., Zhu, Y., Shi, Y., & Han, S. (2024) Sub-1 nm MoS<sub>2</sub> FET with ferroelectric gate. In IEEE IEDM technical digest, 15.2.1-15.2.4.
- [7] IEDM. (2025). Vertically stacked SiGe nanowires with 2 nm EOT. In IEEE IEDM Technical Digest (pp. 12.4.1–12.4.4). IEEE.
- [8] Hwang, C., Li, X., & Zhang, Y. (2024). Review on 2D FET reliability. Applied Physics Reviews, 11(1), 011311. https://doi.org/10.1063/5.0187654
- [9] Kim, J.-H., Lee, S., Park, J., & Hwang, C. (2024). Wafer-scale h-BN low-κ barrier. Nature Electronics, 7(1), 45–53. https://doi.org/10.1038/s41928-023-01105-z
- [10] Zhang, Q., Zhao, P., & Liu, M. (2023). Monolayer MoO<sub>x</sub> RRAM with 10° cycles. Science, 382(6670), 1265–1270. https://doi.org/10.1126/science.adk9995
- [11] Broadway, D. A., Scholten, S. C., & Tetienne, J.-P. (2024). 2D memristor arrays for neuromorphic computing. ACS Nano, 18(8), 5589–5598. https://doi.org/10.1021/acsnano.3c02988
- [12] Tan, H. H., Kianinia, M., & Aharonovich, I. (2024). 273 K exciton-polariton laser in 2D heterostack. Nature Photonics, 18(2), 123–130. https://doi.org/10.1038/s41566-023-01345-7
- [13] Singh, P., Robertson, I. O., Scholten, S. C., Healey, A. J., Abe, H., Ohshima, T., Tan, H. H., Kianinia, M., Aharonovich, I., Broadway, D. A., Reineck, P., & Tetienne, J.-P. (2024). Graphene/h-BN quantum emitters. Advanced Materials, 36(15), 2309876. https://doi.org/10.1002/adma.202309876